Improved Finite Element Simulation of Excavation in Elastic and Elasto-Plastic Geologic Media

K. G. Sharma
Professor
Department of Civil Engineering
Indian Institute of Technology
New Delhi-110 016, India
Phone: 011-6591190
Fax: 011-6581117
E-mail: kgsharma@civil.iitd.ernet.in

A. Varadarajan
Professor
Department of Civil Engineering
Indian Institute of Technology
New Delhi-110 016, India
Phone: 011-6591192
Fax: 011-6581117
E-mail: avrajan@civil.iitd.ernet.in

C. S. Desai
Regent's Professor
Department of Civil Engineering & Engineering Mechanics
University of Arizona
Tucson, AZ85721, USA
E-mail: csdesai@engr.arizona.edu

ABSTRACT

An improved finite element based numerical procedure has been presented for simulation of multi-stage excavation in elastic and elasto-plastic geologic media. Numerical examples demonstrate that the principle of uniqueness is satisfied for the linear elastic case. In the case of elasto-plastic analysis using the Tresca yield criterion, the solution compares closely with the closed-form solution.

1. INTRODUCTION

One of the important attributes of the finite element method when applied to problems of geotechnical engineering is the facility it offers for the simulation of construction history. Two of the important simulations in the construction history involve placement of fill and simulation of excavation. In the present paper, simulation of excavation is considered.

In excavation problems, the construction history is defined by the stages in which the excavation is carried out and supports, if any, are introduced. The early numerical methods for simulating excavations (Goodman and Brown, 1963; Duncan and Dunlop, 1969; Clough and Duncan, 1969; Duncan and Chang, 1970; Dunlop and Duncan, 1970; Clough and Duncan, 1971; Desai and Abel, 1972) were based on the hypothesis of a stress-free surface resulting from the removal of material above the surface. Ishihara (1970) postulated that there exists a unique solution (i.e. the final stresses and displacements must be) independent of the sequence of excavation for a linear elastic material and time independent problem. The excavation simulation algorithms proposed by Christian and Wong (1973) and Clough and Mana (1976) do not satisfy the uniqueness principle (Ishihara, 1970).

Chandrasekaran and King (1974) have described a simple procedure for simulating excavations in soil media, which satisfies the uniqueness requirement. This procedure avoids the use of element stresses and is strictly applicable to elastic materials.

Desai and Sargand (1984) proposed a hybrid method for calculating nodal forces to overcome the violation of the uniqueness requirement but at the cost of added analytical complexity. Ghaboussi and Pecknold (1984) demonstrated the validity of the uniqueness principle by using the principle of virtual work over the appropriate domain of interest. Sharma et al. (1985) used "air" elements for the excavated elements in an algorithm that satisfied the uniqueness requirement.

Borja et al. (1989) proposed a finite element formulation based on variational method for simulating excavation in elasto-plastic soils, which satisfies the uniqueness requirement. They used infinitesimal stiffness for the removed elements. Comodromos et al. (1993) proposed a multi-stage finite element algorithm for excavation in elasto-plastic soils using the principle of virtual work. After the assemblage of the global stiffness matrix and load vector for each excavation stage, the static condensation procedure is employed to reduce the number of element degrees-of-freedom corresponding to the removed nodes.

The objective of this paper is to present an efficient finite element based numerical procedure for simulating multi-stage excavation in elasto-plastic geologic media. This procedure overcomes the limitations of the algorithms proposed by various researches cited above.

2. GENERAL FINITE ELEMENT FORMULATION FOR EXCAVATION SIMULATION

The method of excavation simulation consists of a series of steps (stages), each step representing the removal of one lift of the stressed material from a continuous body. The procedure for one-step excavation is illustrated in Fig.1. Figure 1(a) shows an initial stressed body of soil or rock from which the shaded portion A is to be excavated. The remaining portion is labelled as B.

The traction, t_i, exerted by region A on region B in the initially stressed body is shown in Fig. 1(b). Now the excavation process involves removing the elements and stiffness of portion A and traction, t_i from the portion B in Fig. 1(b). This is done by applying to the portion B traction $-t_i$ (equal and opposite to t_i) as shown in Fig. 1(c). This results in the stress free excavation surface abc. Using the stiffness of portion B and traction $-t_i$, incremental displacements, strains and stresses are obtained and these are added to the original values for the portion B.

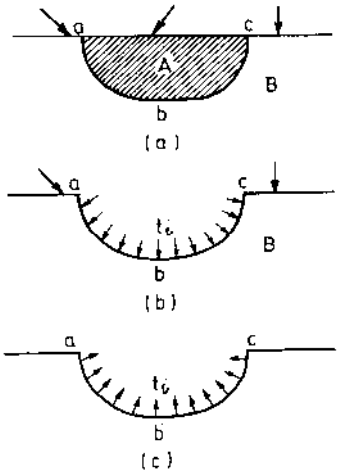

Fig. 1: The excavation process

In the conventional procedure, the equivalent nodal forces are determined by numerical integration or lumping the computed element stresses along element boundaries lying on the excavated surfaces. Unfortunately, this procedure does not yield nodal forces which are consistent (in the finite element context) with the element stresses they are supposed to represent, e.g. the errors reported by Christian and Wong (1973) are due to the inconsistent determination of these nodal forces.

To overcome the above limitations, various researchers (Ghaboussi and Pecknold, 1984; Sharma et al., 1985; Borja et al., 1989; Comodromos et al., 1993) have given consistent general formulation for multi-stage simulation of excavation. They have proposed different algorithms to account for the excavated elements. The general formulation and the disadvantages of the algorithms adopted by various researchers are briefly presented in the following.

Let {P} be the external load vector due to body forces, concentrated loads, and surface pressures. {F} is the internal nodal resisting force vector computed from element stresses $\{\sigma\}$ as

$$\{F\}=\sum_{e=1}^{m}\theta_e\int_{Ve}[B]^T\{\sigma\}dV \qquad (1)$$

where [B] is the strain-displacement matrix, $\{\sigma\}$ is the stress vector and m is the total number of elements. In Eq. (1), θ_e is an indicator which has value zero for the elements to be removed (excavated) and unity for the remaining elements. Thus θ_e will be equal to zero for the elements of region A and equal to unity for the elements of region B (Fig. 1). Therefore, the summation is taken over the relevant group of elements (e.g. for the elements of region B). Equation (1) is evaluated by Gaussian integration and it provides a consistent relation between nodal forces and element stresses on the excavated surface.
A residual nodal load vector {R} is defined as

$$\{R\} = \{P\} - \{F\} \tag{2}$$

The incremental equilibrium equations for increment, i, can be written as

$$[K_{ti}]\ \{dr_i\} = \{dP_i\} + \{R_i\} = \{dQ_i\} \tag{3}$$

where $[K_{ti}]$ is the tangent stiffness matrix, $\{dr_i\}$ is the incremental displacement vector, $\{dP_i\}$ is the incremental load vector (= $\{P_i\}$ - $\{P_{i-1}\}$), $\{R_i\}$ is the residual load vector (= $\{P_{i-1}\}$ - $\{F_{i-1}\}$) and $\{dQ_i\}$ is the net incremental load vector.

For a system which is exactly in equilibrium, $\{R_i\}=0$. In nonlinear analysis, iterations are carried out until norm of $\{R_i\}$, $\|\{R_i\}\|$ is zero to within a small tolerance. Displacements, strains and stresses are then updated as follows:

$$\begin{aligned} \{r_i\} &= \{r_{i-1}\}+\{dr_i\} \\ \{\varepsilon_i\} &= \{\varepsilon_{i-1}\}+\{d\varepsilon_i\} \\ \{\sigma_i\} &= \{\sigma_{i-1}\}+\{d\sigma_i\} \end{aligned} \tag{4}$$

For i =1 (i.e. first stage of excavation), the insitu stress vector $\{\sigma_o\}$ is substituted in Eq.(1) to compute $\{F_o\}$. Thus $\{\sigma_o\}$ is to be computed before the start of the excavation procedure. The computation procedure for insitu stresses is given in Appendix I.

In Eqs. (1) and (3), the load vector {F} and tangent stiffness matrix $[K_t]$ are calculated by taking the summation over the existing elements. Thus the excavated elements up to a particular stage do not contribute to {F} and {K}. This is achieved by deactivation of elements (by assuming $\theta_e = 0$). Some of the excavated (deactivated) elements, which represent the support (shotcrete lining, reinforcement etc.) can be reactivated later when required in a particular sequence of excavation.

2.1 Excavated Region

There are two ways to account for the excavation of elements.

(a) The elements in the excavated region are assumed to be “air” elements, i.e. their contribution to the global stiffness matrix is reduced to almost

zero. This can be done by reducing the Young's modulus of elements in the excavated region to a very low value (say 10^{-6} of the original value) leading to infinitesimal stiffness matrix for the removed elements. This procedure has been followed by Christian and Wong (1973), Clough and Mana (1976), Sharma et al. (1985), Chandrasekaran and King (1974), and Borja et al. (1989). The inclusion of infinitesimal stiffness matrix for the removed elements has two disadvantages (Comodromos et al., 1993):

(i) It violates the principle of virtual work arising from the contribution of the excavated elements to the equilibrium solution process.
(ii) The global stiffness matrix has infinitesimal pivots corresponding to the removed nodes, resulting in a considerable numerical error during the solution process.

(b) From the original mesh of the body, the elements and nodes to be removed are deactivated, i.e. their contributions to the global stiffness matrix and load vector are suppressed. Ghaboussi and Pecknold (1984) and Comodromos et al. (1993) have used this procedure. To eliminate the degrees-of-freedom corresponding to the removed (excavated) nodes, partitioning method and static condensation procedure is employed by Ghaboussi and Pecknold (1984) and Comodromos et al. (1993), respectively. At each excavation stage, an assemblage of the global stiffness matrix and force vector is carried out and then the matrix partitioning or static condensation is done to obtain the equilibrium equations for the remaining domain (after excavation at each stage). This results in larger computer storage and computation time.

3. PROPOSED FINITE ELEMENT ALGORITHM

To overcome the disadvantages of the finite element algorithms given above, a modified finite element algorithm is proposed. The steps for the proposed algorithm are as follows.

Step 1: Set $\theta_e = 1$ for all the elements of the body.

Step 2: Calculate the insitu stresses $\{\sigma_0\}$ at Gauss points of the elements of the body, following the procedure outlined in Appendix I.

Step 3: Calculate the internal nodal resisting force vector $\{F_o\}$ using Eq. (1).

$$\{F_o\} = \sum_e \int_{Ve} [B]^T \{\sigma_0\} dV \tag{5}$$

Step 4: Set the external nodal load vector $\{P_o\} = \{F_o\}$, with this the body is in equilibrium with insitu stresses and the residual load vector {R} of Eq. (2) is zero.

Step 5: For each sequence of excavation i

(i) Apply external load increment $\{dP_i\}$, if any, to the body and add it to the external load vector {P},

$$\{P_i\} = \{P_{i-1}\} + \{dP_i\} \tag{6}$$

(ii) Delete the elements and nodes excavated in this sequence. The deleted elements are assigned $\theta_e = 0$. Thus the elements are deactivated and will not be included in the assembly process of stiffness matrix [K] and in the summation of Eq. (1).

Similarly the deleted nodes are also deactivated and they are allocated full fixity in both x and y directions. *In the present algorithm, the equation numbers are redefined eliminating those degrees-of-freedom for the nodes having fixity in one or both directions. Thus the restrained degrees-of freedom in the original body and corresponding to the deleted (deactivated) nodes due to excavation are eliminated. The limitation of earlier finite element formulations that assumed 'air' elements and that involve matrix and vector partitioning or static condensation are eliminated in the present algorithm. With the deletion of the restrained degrees-of-freedom, the effective number of equations is significantly reduced, resulting in saving in computer storage and time.*

(iii) If insitu stresses are due to gravity (Appendix I), calculate the equivalent nodal load vector $\{Q_{bi}\}$ due to gravity of the excavated elements as

$$\{Q_{bi}\} = \sum_e \int_{Ve} [N]^T \{\overline{X}\} dV \tag{7}$$

where [N] is shape function matrix and $\{\overline{X}\}$ is body force intensity vector with $\{\overline{X}\} = \begin{Bmatrix} 0 \\ -\gamma \end{Bmatrix}$ for a two-dimensional problem and γ is the unit weight of the material.

The summation is taken over the excavated elements. Then define,

$$\{Pi\} = \{Pi\} - \{Q_{bi}\} \tag{8}$$

Skip this step in case of uniform insitu stresses.

(iv) Calculate the load $\{S_i\}$ on excavated surface as

$$\{S_i\} = \{P_i\} - \sum_e \theta_e \int_{Ve} [B]^T \{\sigma\} dV \quad (9)$$

where summation is taken over the remaining elements. The load vector $\{S_i\}$ represents the load on the excavated surface (= $-t_i$ of Fig. 1).

(v) Set $\{P_i\} = \{P_i\} - \{S_i\}$ (10)

(vi) Divide the load vector $\{S_i\}$ into increments, which can be uniform or non-uniform. This is done by defining the load factors α_j. The load vector $\{S_i\}$ is multiplied by load factor α_j to obtain the incremental load vector for jth increment. Since multiplication factors must sum up to unity, $\sum_j \alpha_j = 1$. The load factors α_j can be uniform or non-uniform depending upon whether load increments are uniform or non-uniform.

(vii) For each increment, j

$$\{P_i\} = \{P_i\} + \alpha_j \{S_i\} \quad (11)$$

$$\{dQ_j\} = \{P_i\} - \sum_e \theta_e \int_{Ve} [B]^T \{\sigma\} dV \quad (12)$$

$$[K_{ij}] [dr_j] = \{dQ_j\} \quad (13)$$

Solve for displacements $\{dr_j\}$ and then compute incremental strains and stresses. Displacements, strains and stresses are updated using Eq. (4). Iterations are carried out until convergence is obtained. For the elasto-plastic finite element analysis, the procedure as explained by Desai et al. (1991) in detail for hierarchical models is used. This procedure is also applicable for other yield criteria.

Step (vii) is followed for all the increments and step 5 is repeated for all the sequences of excavation.

It may be noted that some of the deactivated elements, which form concrete or shotcrete lining or reinforcement elements can be reactivated later, when required in a particular sequence of excavation. The algorithm provides for both deactivation and reactivation of elements and nodes and also for change of properties by assigning different material type to the reactivated elements.

4. ANALYSIS AND RESULTS

The proposed algorithm of Section 3 has been implemented in computer program DSC-SST-2D (Desai, 1999) developed for 4-noded and 8-noded solid elements in FORTRAN-90 language. The program has been verified by comparing predictions with closed-form solutions and other numerical schemes for problems in simulation of excavation sequences. The predictions satisfy the uniqueness principle (Ishihara, 1970) for linear elastic analysis. The analyses and results of three typical problems are presented herein.

The first example deals with a numerical patch test on a linear elastic one-dimensional excavation problem solved by Clough and Mana (1976) and Desai and Sargand (1984). The second example concerns a two-dimensional plane strain excavation problem which has been solved for linear elastic and elasto-plastic behaviour. These two examples have also been analysed by Comodromos et al. (1993). The third problem is related to a deep circular tunnel.

4.1 Example 1: Simulation of one-dimensional excavation

Clough and Mana (1976) analysed a linear elastic one-dimensional excavation problem (Fig. 2) using 8-noded elements in which the upper half (20 m) of the material was excavated using one and eight steps. The parameters used in the analysis are:

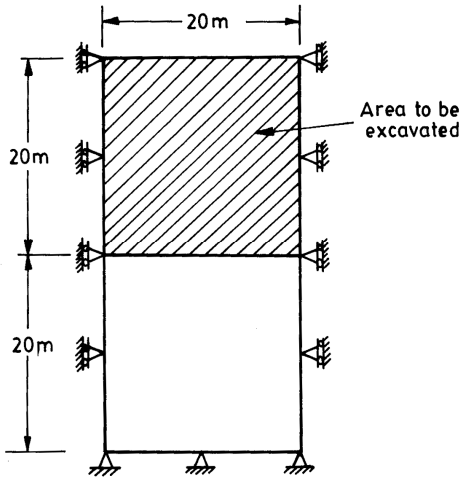

Fig. 2: One-dimensional excavation problem

Young's modulus,	$E = 10000$ t/m^2
Poisson's ratio,	$\nu = 0.2$
Unit weight,	$\gamma = 1$ t/m^3
In-situ stress ratio,	$K_o = 0.5$

Desai and Sargand (1984) solved the same problem using hybrid method by simulating the excavation of upper half by one element. Taking into account

the boundary conditions (Fig. 2) and plane strain condition the exact solution for this problem for vertical stress, σ_y, can be derived as

$$\sigma_y = \frac{E}{(1+\nu)} + \frac{\nu E \varepsilon_y}{(1+\nu)(1-2\nu)} \tag{14}$$

where ε_y is the vertical strain.

When upper half (Fig. 2) is excavated, a surface traction of σ_y = 20 t/m^2 is applied substituting it in Eq. (14), ε_y is computed as 1.8 x 10^{-3}. Then the vertical displacement v at the excavated surface is 1.8 x 10^{-3} x 20 m = 0.036 m = 3.6 cm.

The same problem was analysed using the proposed algorithm and program DSC-SST-2D by one and four excavation stages (Fig. 3). Element 2 is excavated in Fig. 3a and elements 2, 3, 4 and 5 are excavated in Fig. 3b by removing one element in each sequence. The results obtained were identical providing a displacement of 3.6 cm for the nodes on the excavated surface. The predicted values compare exactly with the closed-form solution and the predicted value is independent of number of sequences, thus satisfying the uniqueness requirement, Ishihara (1970). The same results are obtained when 4-noded elements are used in Fig. 3.

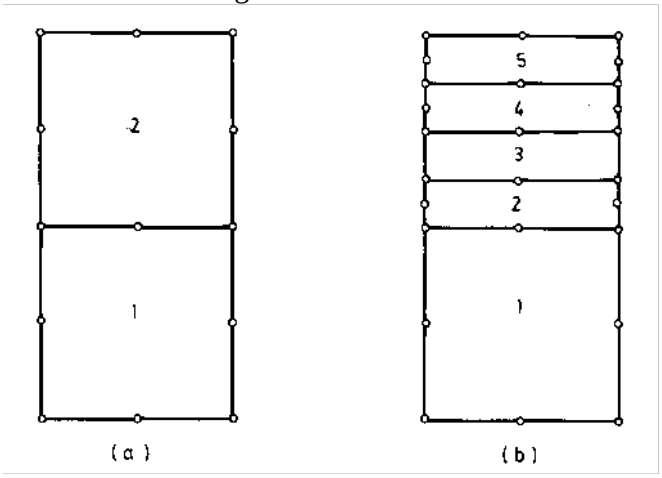

Fig. 3: Finite Element Mesh for one-dimensional excavation
(a) Single stage (b) Four stage

4.2 Example 2: Plane Strain Excavation in Elasto-Plastic Material

The problem of two-dimensional plane strain excavation analysed by Comodromos et al. (1993) has been considered. The mesh is shown in Fig. 4. It has 72, eight-noded elements and 251 nodes. Nodes along the bottom boundary are restrained in both directions whereas the nodes along the two (left and right) vertical boundaries are restrained in horizontal direction. The elements in the upper right hand corner, bounded by thick line are excavated in one and three stages.

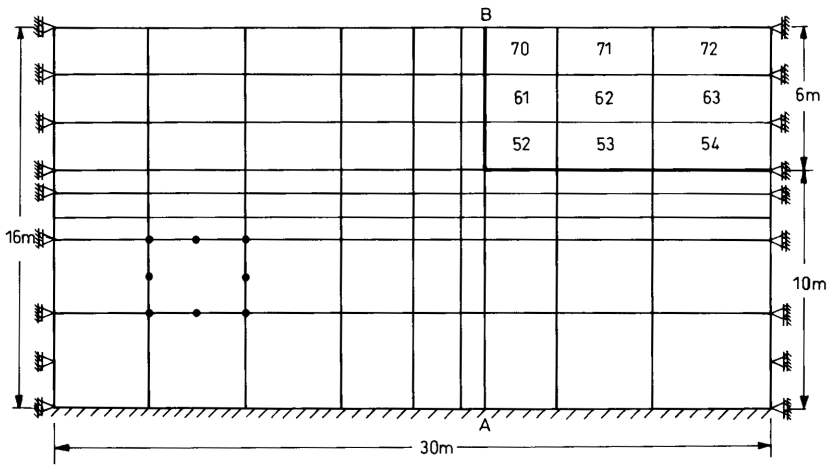

Fig. 4: Finite element mesh for two-dimensional plane strain open excavation

The analyses have been carried out for linear elastic behaviour and elasto-plastic behaviour using Drucker-Prager yield criterion given by

$$f = aJ_1 + \sqrt{J_{2D}} - k = 0 \tag{15}$$

where J_1 denotes the first invariant of stress tensor, J_{2D} is the second invariant of deviatoric stress tensor and a and k are material constants.

The parameters used in the two analyses are:

Unit weight, $\gamma = 19.8$ kN/m^3
Bulk modulus, K = 4700 kPa
Shear modulus, G = 2200 kPa
Insitu stress ratio, $K_o = 0.9$
Drucker-Prager parameter, a = 0.25
Drucker-Prager parameter, k = 10 kPa

Single stage and three stage excavation analyses were performed. In the first case, elements 52-54, 61-63 and 70-72 (9 elements) were removed simultaneously, while in the second case, three-step layer by layer excavation was considered in which elements 70-72, 61-63 and 52-54 are removed sequentially.

Figure 5 shows the horizontal displacement profile of the vertical boundary of excavation line AB (shown in Fig. 4) for the two cases from linear elastic analysis. It can be seen that the resulting final profile for both single and three-step analyses is identical, a fact that verifies the uniqueness requirement.

The above analyses were carried out by considering elasto-plastic soil behaviour with the Drucker-Prager yield criterion. The horizontal displacement profiles are shown in Fig. 6. A very small difference between the two final

profiles is observed in numerical values (maximum difference of less than 1%), but it is not visible in Fig. 6. These results compare closely with those by Comodromos et al. (1993).

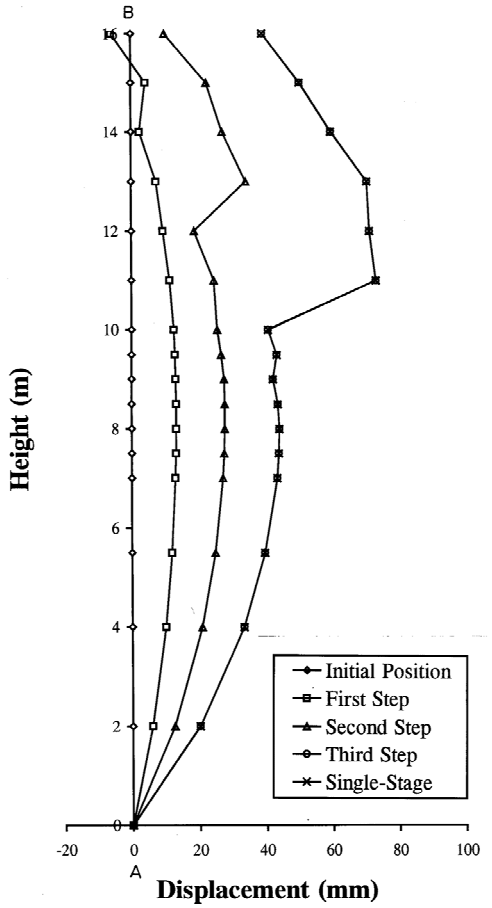

Fig. 5: Horizontal displacement profile along line AB due to linear elastic analysis (Example 2)

4.3 Example 3: Excavation of a Deep Circular Tunnel

A circular tunnel of 8.0 m diameter located at a depth, h, of 300 m below ground level is to be excavated. It is considered to be deep tunnel with uniform insitu stress condition. The rock medium is considered to be biotite gneiss. The analyses have been carried out for linear elastic behaviour and elasto-plastic behaviour using Tresca yield criterion. The material properties are as follows:

Young's modulus, $E = 4.48 \times 10^5$ kPa
Unit weight, $\gamma = 29.4$ kN/m^3
Poisson's ratio, $\nu = 0.18$
Height of over burden (h) = 300 m
Insitu stress ratio, $K_o = 1$
Tresca strength constant, k = 4150 kPa

Corresponding to h = 300 m, the uniform insitu stresses are (Eqs. I.1- I.3 in Appendix - I).

$$\sigma_{vo} = \gamma h = 8820 \text{ kPa}$$
$$\sigma_{ho} = K_o \sigma_{vo} = 8820 \text{ kPa}$$
$$\tau_{vho} = 0$$

Since the problem is symmetric about both x and y axes, only quarter section of tunnel with surrounding rock is discretised. The mesh is shown in Fig. 7. It has 35, 8-noded elements and 134 nodes. Elements 1 and 2 are excavated in one step. In Fig. 7, the arcs are taken at radius of 4.0, 4.2, 4.5, 5, 5.75, 7, 9, 13, 20, 32, 50 and 80 m and radial lines at angles of 0, 30, 60 and 90 degrees are considered.

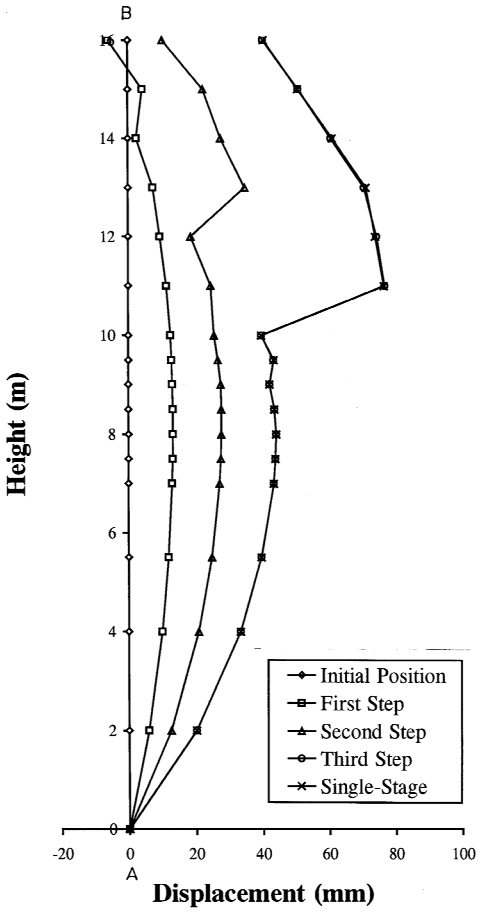

Fig. 6: Horizontal displacement profile along line AB due to elasto-plastic analysis (Example 2)

Both linear elastic and elasto-plastic analyses are carried out using plane strain idealization.

(a) Linear Elastic Analysis

Pender (1980) has given closed form solution for displacements and stresses for a circular tunnel for excavation in a uniform insitu stress field considering linear elastic behaviour. The equations for $K_o = 1$ condition are as follows:

$$u = \frac{1+\nu}{E}\frac{pa^2}{r} \tag{16}$$

$$\sigma_r = p\,(1 - a^2 / r^2) \tag{17}$$

$$\sigma_\theta = p\,(1 + a^2 / r^2) \tag{18}$$

where p is the uniform insitu stress, a is the radius of tunnel and r is any radial distance, u is the radial displacement and σ_r and σ_θ are radial and circumferential stresses respectively. The stresses σ_r and σ_θ are the minor (σ_3) and major (σ_1) principal stresses respectively as shear stress $\tau_{r\theta} = 0$.

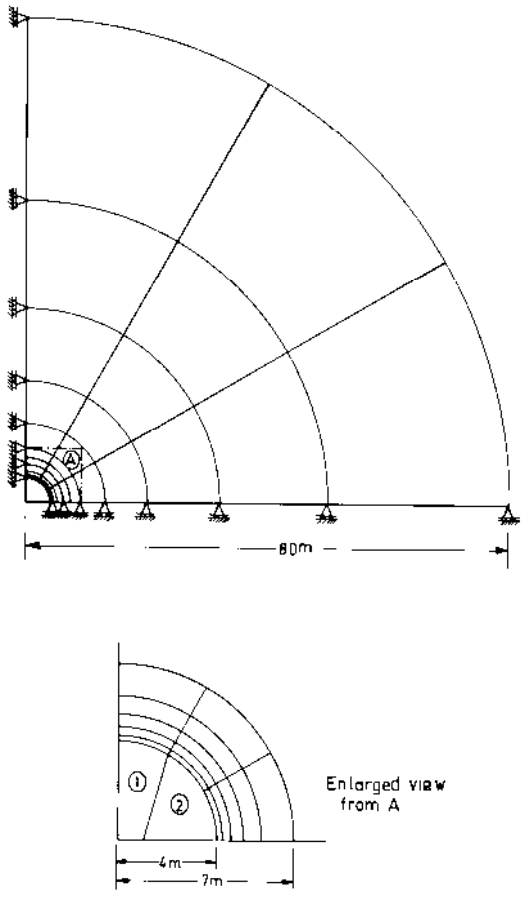

Fig. 7: Finite element mesh for circular tunnel

Table 1: Radial Displacements (Elastic Analysis)

Radial distance (m)	Radial displacement (mm)	
	Closed-form, Eq. (16)	FEM
4.00	92.93	93.59
4.20	88.50	88.91
4.50	82.60	83.00
5.00	74.34	74.74
5.75	64.64	65.04
7.00	53.10	53.52
9.00	41.30	41.77
13.00	28.59	29.17
20.00	18.59	19.40
32.00	11.62	12.85
50.00	7.43	9.32
80.00	4.65	7.64

Table 2 : Principal Stresses (Elastic Analysis)

Radial distance (m)	Principal stresses (kPa)			
	Closed-form, Eqs. (17)-(18)		FEM	
	σ_1	σ_3	σ_1	σ_3
4.04	17458.8	181.2	17500.3	183.7
4.16	16985.6	654.4	17026.0	658.3
4.26	16585.8	1054.2	16625.5	1058.7
4.44	15991.3	1648.7	16029.4	1654.8
4.61	15474.5	2165.5	15512.0	2172.3
4.89	14712.7	2927.3	14747.7	2936.5
5.16	14124.6	3515.4	14159.4	3524.9
5.59	13334.8	4305.2	13366.5	4317.7
6.01	12722.6	4917.4	12754.9	4929.3
6.73	11931.1	5708.9	11959.1	5725.1
7.42	11382.0	6258.0	11411.8	6272.4
8.58	10738.6	6901.4	10763.6	6920.6
9.84	10276.3	7363.7	10305.1	7379.1
12.15	9775.5	7864.5	9797.4	7886.8
14.48	9493.3	8146.7	9519.5	8164.7
18.52	9231.5	8408.5	9253.0	8431.3
22.53	9097.9	8542.1	9122.1	8562.1
29.46	8982.6	8657.4	9004.3	8680.0
35.80	8930.1	8709.9	8952.9	8731.3
46.19	8886.1	8753.9	8908.1	8776.1
56.33	8864.5	8775.5	8886.9	8797.3
73.65	8846.0	8794.0	8868.0	8816.2

Table 3 : Principal Stresses (Elasto-Plastic Analysis)

Radial distance (m)	Principal stresses (kPa)			
	Closed-form, Eqs. (21)-(24)		FEM	
	σ_1	σ_3	σ_1	σ_3
4.04	8386.2	86.2	8387.2	87.2
4.16	8619.9	319.9	8621.0	321.0
4.26	8828.2	528.2	8829.3	529.3
4.44	9158.8	858.8	9159.8	859.8
4.61	9469.2	1169.2	9470.3	1170.3
4.89	9973.7	1673.7	9974.7	1674.7
5.16	10410.0	2110.0	10411.3	2111.3
5.59	11079.1	2779.1	11080.0	2780.0
6.01	11683.8	3383.9	11685.5	3385.5
6.73	11624.5	4324.5	12625.1	4325.1
7.42	12534.3	5105.7	12596.9	5107.5
8.58	11601.5	6038.5	11652.3	6052.1
9.84	10931.2	6708.8	10984.2	6720.2
12.15	10205.2	7434.8	10244.3	7460.1
14.48	9796.1	7843.9	9839.4	7865.1
18.52	9416.6	8223.4	9450.9	8253.5
22.53	9222.9	8417.1	9260.2	8444.2
29.46	9055.7	8584.3	9088.5	8615.9
35.80	8979.6	8660.4	9013.7	8690.7
46.19	8915.9	8724.1	8948.4	8756.0
56.33	8884.5	8755.5	8917.5	8786.9
73.65	8857.7	8782.3	8890.0	8814.4

Linear elastic analysis of tunnel using the mesh in Fig. 7 was carried out in single step by removing elements 1 and 2. The results for displacements and stresses are presented in Tables 1 and 2. The results of closed-form solutions are also tabulated in these tables for comparison. There is a close agreement between the two results. The small discrepancy can be due to the non-simulation of infinite extent of the rock medium.

(b) Elasto-plastic analysis

Obert and Duvall (1967) have presented the derivation for stresses for elasto-plastic analysis of a circular tunnel for uniform insitu stress field with K_o=1 condition considering Tresca yield criterion:

$$\sigma_1 - \sigma_3 = 2k \qquad (19a)$$

or $$\sigma_\theta - \sigma_r = 2k \qquad (19b)$$

where σ_1 and σ_3 are major and minor principal stresses respectively and k is the strength constant. The equations for stresses and the radial distance, c up to the boundary between the plastic and elastic zones are as follows:

$$c = a \exp\left(\frac{p-k}{2k} \right) \tag{20}$$

Plastic zone ($a \le r \le c$)

$$\sigma_r = 2k \ln (r/a) \tag{21}$$

$$\sigma_\theta = 2k [1 + \ln (r/a)] \tag{22}$$

Elastic zone ($r \ge c$)

$$\sigma_r = p\left[1 - \frac{ka^2}{pr^2} \exp\left(\frac{p-k}{k} \right) \right] \tag{23}$$

$$\sigma_\theta = p\left[1 + \frac{ka^2}{pr^2} \exp\left(\frac{p-k}{k} \right) \right] \tag{24}$$

Using p = 8820 kPa and k = 4150 kPa, c is determined as 7.02 m. Thus the zone within $4 \le r \le 7.02$ is plastic and zone with $r \ge 7.02$ m is elastic.

Elasto-plastic analysis of the tunnel using mesh in Fig. 7 was carried out in single step by removing elements 1 and 2. The yield zone from finite element analysis develops from element 3 to 17 i.e. up to radius of 7 m. The results for stresses are presented in Table 3 along with those from Eqs. (21) – (24). The two results compare closely. The small discrepancy can be due to the non-simulation of infinite extent of the rock medium.

5. CONCLUSIONS

A finite element formulation for simulating multi-stage excavation in elasto-plastic geologic medium has been presented. A detailed algorithm is presented which can be easily implemented in any computer code. The excavated elements and nodes are eliminated during assembly in this algorithm, thus it is not necessary to use "air" elements, static condensation and matrix partitioning as it was done in previous processes by others. Due to this, the algorithm is very efficient and accurate.

Numerical examples demonstrate that the proposed algorithm satisfies the uniqueness requirement for elastic excavation problems. In the case of elasto-plastic analysis (example 2) one –stage and three-stage analyses give slightly different results with maximum difference of less than 1.0%. In practice, multi-stage excavation should be used to obtain realistic and accurate solutions for elasto-plastic geologic medium.

In case of deep circular tunnel (example 3) the predicted results match closely with the closed form solutions. The small discrepancy can be due to the non-simulation of infinite extent of the rock medium.

References

Borja, R.I., Lee, S.R. and Seed, R.B. (1989). Numerical simulation of excavation in elasto-plastic soils, Int. J. Numer. Anal. Methods in Geomech., 13, pp. 231-249.

Chandrasekaran, V.S. and King, G.J.W. (1974). Simulation of excavation using finite elements, J. Geotech. Engg. Div., ASCE, 100, pp. 1086-1089.

Christian, J.T. and Wong, I.H. (1973). Errors in simulation of excavation in elastic media by finite elements, Soils and Foundations, 13, pp. 1-10.

Clough, G.W. and Duncan, J.M. (1969). Finite element analyses of port Allen and old river locks, University of California, Berkeley, Report TE-69-3.

Clough, G.W. and Duncan, J.M. (1971). Finite element analyses of retaining wall behaviour, J. Soil Mech. Found. Div., ASCE, 97, pp. 1657-1673.

Clough, G.W. and Mana, A.I. (1976). Lessons learned in finite element analysis of temporary excavations, Proc., 2nd Int. Conf. on Numer. Methods in Geomech., Blacksburg, VA.

Comodromos, E., Hatzigogos, Th. and Pitilakis, K. (1993). Multi-stage finite element algorithm for excavation in elasto-plastic soils, Computers and Structures, 46, pp. 289-298.

Desai, C.S. (1999). Computer Code DSC-SST2D for static, dynamic, creep and thermal analysis: solid, structure and soil-structure problems, Tucson, AZ.

Desai, C.S. and Abel, J.F. (1972). Introduction to the finite element method, Van Nostrand Reinhold Co., New York.

Desai, C.S. and Sargand, S. (1984). Hybrid FE procedure for soil-structure interaction, J. Geotech. Engg. Div., ASCE, 110, pp. 473-486.

Desai, C.S., Sharma, K.G., Wathugala, G.W. and Rigby, D.B. (1991). Implementation of hierarchical single surface δ_0 and δ_1 models in finite element procedure, Int. J. Numer. Anal. Methods in Geomech., 15, pp. 649-680.

Duncan, J.M. and Chang, C.Y. (1970). Nonlinear analysis of stress and strain in soils, J. Soil Mech. Found. Div., ASCE, 96, pp. 1629-1653.

Duncan, J.M. and Dunlop, P. (1969). Slopes in stiff fissured clays and shales, J. Soil Mech. Found. Div., ASCE, 95, pp. 81-104.

Dunlop, P. and Duncan, J.M. (1970). Development of failure around excavated slopes, J. Soil Mech. Found. Div., ASE, 96, 471-493.

Ghaboussi, J. and Pecknold, D.A. (1984). Incremental finite element analysis of geometrically altered structures, Int. J. Numer. Meth. Engg., 20, pp. 2051-2064.

Goodman, L.E. and Brown, C.B. (1963). Dead load stresses and the instability of slopes, J. Soil Mech. Found. Div., ASCE, 89, pp. 103-134.

Ishihara, K. (1970). Relations between process of cutting and uniqueness of solutions, Soils and Foundations, 10, pp. 50-65.

Obert, L. and Duvall, W.I. (1967). Rock Mechanics and the design of structures in rock, John Wiley and Sons.

Pender, M.J. (1980). Elastic solutions for a deep circular tunnel, Geotechnique, pp. 216-222.

Sharma, K.G., Varadarajan, A. and Srivastava, R.K. (1985). Elasto-viscoplastic finite element analysis of tunnels, Proc. 5th Int. Conf. on Numer. Meth. in Geomech., Nagoya (Japan), 2, pp. 1141-1148.

APPENDIX - I

INSITU STRESSES

Insitu stresses in the ground are due to the gravity stresses and past tectonic forces. There are two options for computing insitu stresses, depending upon the type of problem to be analysed and these are discussed below.

(i) Gravity insitu stresses

The vertical insitu stress σ_{vo} due to gravity is calculated due to the over-burden and lateral insitu stress σ_{h0} is taken as in-situ stress ratio (or coefficient of earth pressure at rest) K_o times the vertical insitu stress. For horizontal ground, insitu shear stress τ_{hv0} is taken as zero. Thus,

$$\sigma_{v0} = \gamma y \quad \text{(I.1)}$$

$$\sigma_{h0} = K_o \sigma_{v0} \quad \text{(I.2)}$$

$$\tau_{hv0} = 0 \quad \text{(I.3)}$$

where γ is the unit weight and y is the overburden depth.

The above equations are applicable for homogeneous continuous body. When the body to be analysed is non-homogeneous, Eqs.(I.1) to (I.3) cannot be used as γ is variable from layer to layer. In this case, finite element analysis of the body is carried out for the gravity forces. The vertical stress from the analysis is taken as σ_{v0} and the lateral and shear stresses are modified using Eqs. (I.2) and (I.3).

(ii) Uniform insitu stresses

For the analysis of deep tunnels, the in-situ stresses are taken as uniform in the body i.e. all the elements will have same insitu stresses. The vertical in-situ stress σ_{v0} is calculated using Eq. (I.1) by taking overburden depth y up to the centre of the tunnel. Then Eqs. (I.2) and (I.3) are used to determine lateral and shear stresses. Thus the stress vector $\{\sigma_o\}$ will be the same in all the elements.